$X\alpha$ scattered-wave calculations for dimers and trimers of tetrathiafulvalene (TTF) and tetracyanoquinodimethane (TCNQ)

F. Herman
IBM Research Laboratory, San Jose, California 95193

D. R. Salahub† and R. P. Messmer
General Electric Company, Corporate Research and Development, Schenectady, New York 12301

(Received 29 March 1977)

$X\alpha$ scattered-wave molecular-orbital (MO) calculations have been carried out for dimers and trimers of tetrathiafulvalene (TTF) and tetracyanoquinodimethane (TCNQ) in the slipped C_{2h} geometry found in crystalline TTF-TCNQ. The MO's of the dimers which are the precursors of the partially filled valence and conduction bands in TTF-TCNQ are found to a good approximation to be simply bonding and antibonding combinations of the highest occupied MO (donor level) in the case of TTF and the lowest unoccupied MO (acceptor level) in the case of TCNQ. When extended basis sets are used, the energy difference between corresponding bonding and antibonding levels (dimer splitting) is 0.24 eV for a TTF dimer and 0.29 eV for a TCNQ dimer. These basis sets include s, p, and d partial waves on C, S, and N atoms, and s and p partial waves on H atoms. When the dimer and trimer levels are fitted to a tight-binding model containing the transfer integral t and the overlap integral S, it is found that S is negligible. The infinite-stack bandwidths W are then equal to twice the dimer splittings and the transfer integrals to half the dimer splittings. The derived TTF and TCNQ bandwidths (0.48 and 0.58 eV, respectively) are consistent with available experimental estimates.

I. INTRODUCTION

There has been considerable interest recently in a number of organic and inorganic solids which have highly anisotropic electrical, optical, and/or magnetic properties.[1] Indeed, some of these materials show behavior which is consistent with one-dimensional models, for example, a metal-insulator transition which is interpreted as being due to a Peierls instability. The three systems which have received the most detailed attention are $K_2Pt(CN)_4Br_{0.3}\cdot 3.2H_2O$ (KCP) (Ref. 2), tetrathiafulvalene-tetracyanoquinodimethane (TTF-TCNQ)[3], and polymeric sulfur nitride (SN_x).[4] In all of these materials, the electrical conductivity is quite high (of the order of 10^2–10^3 $\Omega^{-1}\,cm^{-1}$) for a certain preferred crystallographic direction and much less in perpendicular directions. For these three compounds the anisotropy is greatest for KCP and least for $(SN)_x$.[5]

It is possible to learn a great deal about the electronic structure of these materials by carrying out calculations for the individual molecular units which form these solids, as well as for constituent dimers and trimers. The present authors and their co-workers have previously reported the results of such calculations relevant to KCP (Refs. 6 and 7), TTF-TCNQ (Refs. 8–12), and $(SN)_x$ (Refs. 13 and 14).

In an earlier study of TTF dimers, we found that self-consistent $X\alpha$ scattered-wave calculations led to rough estimates of the bandwidths for the TTF chains in TTF-TCNQ and TTF-$Br_{0.71\text{-}0.76}$.[12] We also demonstrated that the bandwidth is a sensitive function of the stacking geometry. For example, in going from the C_{2h} (slipped) geometry appropriate to TTF-TCNQ to the D_{2h} (eclipsed) geometry appropriate to TTF-$Br_{0.71\text{-}0.76}$, the bandwidth increases by a factor of 4. As a complement to our earlier study of TTF dimers,[12] we report here the results of $X\alpha$ scattered-wave calculations for TTF trimers and TCNQ dimers and trimers, all having the C_{2h} (slipped) geometry appropriate to TTF-TCNQ.

An important outcome of our studies of TTF and TCNQ dimers is that the molecular orbitals of the monomers that give rise to the partially occupied, overlapping valence and conduction bands in solid TTF-TCNQ are disturbed only slightly by formation of the dimers. Consequently, the electronic-energy-band structure of an infinite TTF or TCNQ stack can be determined by using the "relevant" monomer molecular orbitals as fixed (k-independent) basis functions in a tight-binding approximation. For the purpose of this paper, we will ignore interchain coupling and focus our attention on those features of the band structure of TTF-TCNQ that are associated with the TTF and TCNQ intrachain couplings.

Self-consistent dimer calculations are perhaps more descriptive of isolated dimers in solution or in certain crystal structures, such as TTFBr and TTFCl,[15] than of adjacent molecules in uniformly spaced infinite stacks, as in TTF-TCNQ. A

useful approximate description of a dimer or trimer belonging to such a stack can be obtained by constructing *model* dimer or trimer potentials in terms of self-consistent monomer potentials which neglect the small charge redistribution produced by stack formation. The electronic structure of these model dimers and trimers is then determined by performing scattered-wave calculations in a noniterative mode. Much of the present paper is devoted to a consideration of model dimer and trimer scattered-wave calculations for the TTF and TCNQ stacks in TTF-TCNQ.

In order to make contact with the more common linear-combination-of-atomic-orbitals (LCAO) treatments, we introduce a tight-binding model based on intrachain transfer and overlap integrals t and S, respectively. By determining the orbital splittings for the dimers and trimers, it is possible to determine t and S, from which it is further possible to determine the infinite-stack bandwidth, W. As will be seen, our scattered-wave calculations lead to very small values of S. Hence, S can be neglected, and the transfer integral t is given rather accurately by half the dimer splitting ($\Delta_2 = 2t$), and the bandwidth W by twice the dimer splitting ($W = 2\Delta_2 = 4t$).

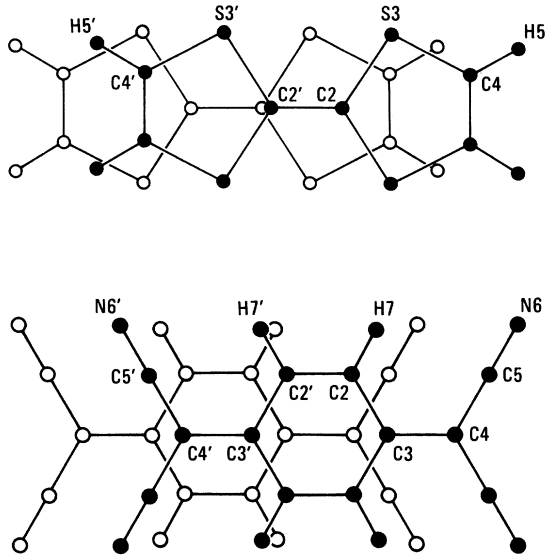

FIG. 1. Molecular structures of TTF (top) and TCNQ (bottom) and their stacking in the TTF-TCNQ crystal. Symmetrically inequivalent atoms are labeled. In the scattered-wave calculations, each atom is surrounded by an overlapping atomic sphere, and all these spheres are in turn surrounded by an externally tangent outer sphere denoted by OUT 1 (not shown).

II. METHOD AND CHOICE OF PARAMETERS

The geometries used for the TTF and TCNQ molecules were taken from x-ray crystal-structure data[16] and idealized so that the monomers have D_{2h} symmetry and the dimers C_{2h} symmetry. The molecular structures of TTF and TCNQ and a schematic diagram of their stacking in the TTF-TCNQ crystal are shown in Fig. 1. The numbering of the atoms used in subsequent discussions is also shown in this figure. The tilt of the molecules with respect to the stacking axis is 24.5° for the TTF stack and 34° for the TCNQ stack; the intermolecular distances are 3.47 and 3.17 Å, respectively.

All the scattered-wave calculations were performed using the overlapping atomic sphere version[8-12] of the method. For simplicity, the exchange parameter α was set equal to 0.75 for all regions of space, as was done in our earlier work on TTF and TCNQ monomers.[8-11] (In some of the calculations α was set equal to 0.77725 inside the hydrogen spheres, but the results for the relevant molecular orbitals are indistinguishable from those obtained using $\alpha = 0.75$ inside these spheres.)

There is experimental evidence[17] that the charge transfer in TTF-TCNQ is roughly one electron per dimer pair, $(TTF\text{-}TCNQ)_2$. Our earlier scattered-wave calculations on TTF dimers[12] and pilot studies of TCNQ dimers both indicated that the dimer splittings are relatively insensitive to the charge state of the monomers. In particular, nearly identical dimer splittings were obtained for $(TTF)_2^0$ and $(TTF)_2^{2+}$, and also for $(TCNQ)_2^0$ and $(TCNQ)_2^{2-}$. In view of the insensitivity of the dimer splitting to the charge state and the uncertainty in the charge transfer, we decided to focus our attention on dimers and trimers formed from neutral monomers.

The atomic radii used for the TTF monomer in the present work are the same as in Ref. 12. For TCNQ we used two different sets, I and II, where set I was obtained using Norman's criterion (see the Appendix), and set II is the same as in the second paper listed under Ref. 8. Although the precise energy separations between successive monomer levels differ slightly for different choices of atomic radii, as previously discussed,[8-10] the order of levels and the general pattern of energy separations remain the same for widely different choices of "chemically reasonable" overlapping atomic-sphere radii. In pilot studies, we found that the dimer splittings of principal interest are also relatively insensitive to such choices of atomic radii.

The only two features of scattered-wave calculations that appear capable of influencing the dimer splittings to a significant degree, say a factor of 2 or more, are (i) whether the calculations are

carried out self-consistently or not; and (ii) the size of the basis set, i.e., the number of partial waves used in the atomic and intersphere regions. (The number of partial waves used in the outer-sphere region is of no importance in this regard.) For purposes of comparison we carried out both self-consistent and non-self-consistent calculations for the dimers. We also studied the effects of using different basis sets on the calculated dimer (and trimer) splittings.

For convenience, we will define three different basis sets: (a) *minimum basis set*: includes s and p waves ($l_{max}=1$) for C, S, and N spheres, and only s waves for H spheres; (b) *intermediate basis set*: same as minimum for TTF, except that d waves are also included for the S spheres (not applicable to TCNQ); and (c) *extended basis set*: includes s, p, and d waves ($l_{max}=2$) for C, S, and N spheres, and only s and p waves for H spheres.

In all the monomer calculations relevant to the present work, the usual choice for the outer-sphere regions was $l_{max}=3$, though virtually the same results were obtained using $l_{max}=4$. For all the dimer and trimer calculations, $l_{max}=2$ was used for the outer-sphere region. In all calculations, the outer sphere was drawn externally tangent to the outermost atomic spheres.

The general strategy of the present study (supplemented by Ref. 12) is outlined below. First, self-consistent scattered-wave solutions were obtained for TTF and TCNQ monomers. Then model calculations were carried out for TTF and TCNQ dimers and trimers using the self-consistent monomer solutions as the starting points. Finally, self-consistent dimer calculations were performed for TTF and TCNQ. We carried out a sufficient variety of calculations using different basis sets and atomic-sphere radii to provide an overall perspective. The model dimer or trimer potentials were constructed by superimposing the atomic potentials obtained from the self-consistent monomer calculations, using the same inter- and outer-sphere potentials for the dimer or trimer as for the monomer. Since the self-consistent monomer solutions depend to some degree on the choice of basis set, we always used the same basis sets for a given series of monomer, dimer, and trimer calculations.

The highest occupied orbital in the donor (TTF) as well as the lowest unoccupied orbital in the acceptor (TCNQ) gives rise to a bonding and an antibounding level in the dimer, as indicated in Fig. 2. In this figure we show, for future reference, the relationships between the energy-level structures of dimers, trimers, ... and infinite stacks. The symmetry correlation between the irreducible representations (IR's) for the monomers (D_{2h}) and the

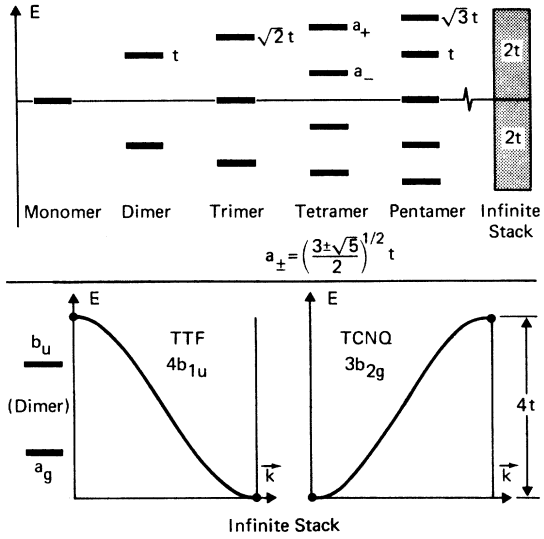

FIG. 2. Comparison of energy levels for monomers, dimers, trimers, etc., indicating their relationship to the energy-level spectrum of an infinite stack. In the upper panel, t denotes the transfer integral, and S, the overlap integral, has been set equal to zero. The band structures of infinite TTF and TCNQ stacks are shown in the lower panel.

dimers and trimers (C_{2h}) is indicated in detail in Fig. 3. The symmetry notation is that of Cotton.[18] The x and y axes lie along the long and short axes of the monomer, and the z axis is perpendicular to the plane of the monomer. For s, p_x, and p_y atomic orbitals the plus and minus signs denote opposite phases in the monomer plane, while for p_z atomic orbitals these signs denote the phase of the upper lobe (above the plane of the monomer). The symmetries of the monomer molecular orbitals are indicated at the top of Fig. 3, and those of the dimers and trimers below. In each of the four lower quadrants, there are three orbitals indicated, two distinguished by plus-minus signs on the central monomer, and the third by no entry (zero) on the central monomer. These three orbitals correspond to the trimer solutions. The dimer solutions can also be read off by ignoring the central monomer. Each detailed figure actually represents two symmetry correlations, one arising from σ monomer orbitals, and another from π monomer orbitals.

For the monomer levels of interest here (TTF $4b_{1u}$ and TCNQ $3b_{2g}$, see Sec. III), the bonding and antibonding dimer levels belong to a_g and b_u (C_{2h}), respectively. In the case of the trimers, the upper and lower levels of a given triplet will always belong to different C_{2h} IR's, while the central level will belong to one or the other of these, depending on the monomer D_{2h} parentage. If the overall trim-

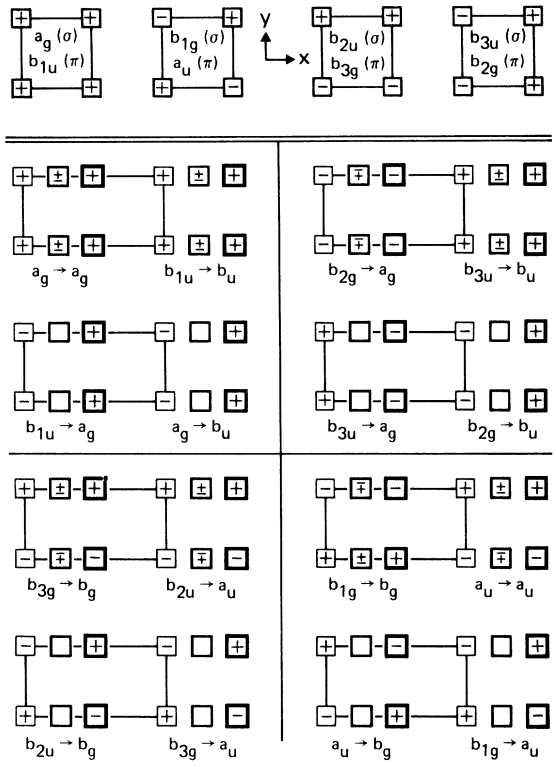

FIG. 3. Symmetry correlation between irreducible representations of monomers (D_{2h}) and dimers and trimers (C_{2h}). The monomers are shown at the top, the trimers (and dimers) below. The topmost member of a trimer is denoted by the bold squares, the bottommost member by the connected squares. The dimers are obtained by ignoring the central members of the trimers.

er (triplet) splitting is very small, it may be difficult to resolve the central level of a triplet from the highest or lowest member of the same triplet. While this may be only a nuisance in model calculations, it can become a serious obstacle operationally in self-consistent trimer calculations, particularly when two monomer levels give rise to nearly-degenerate trimer triplets. Fortunately, we did not find it necessary to do such calculations. Moreover, in the model-trimer calculations, the splittings (within a triplet) were sufficiently large to be readily resolved.

III. RESULTS AND DISCUSSION

A. TCNQ and TTF monomers

The electronic structures of the TCNQ and TTF molecules and some of their ions have been calculated by a variety of quantum-chemical methods: scattered wave,[8-11] semiempirical,[19-23] and *ab initio*.[24,25] Although the detailed numerical values for the various energy levels (and sometimes their

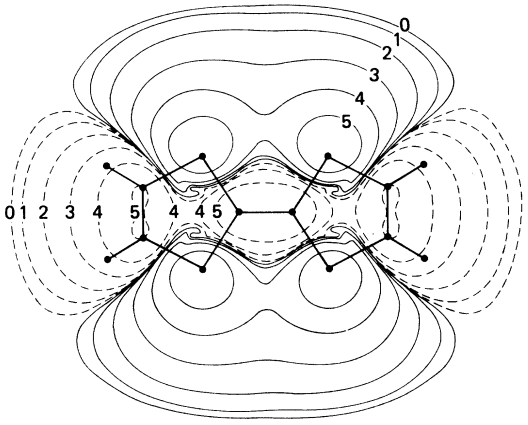

FIG. 4. $4b_{1u}$ molecular orbital for TTF, drawn in a plane $\frac{1}{4}$ of the way between successive molecules in a TTF chain in TTF-TCNQ. Positive and negative values are distinguished by solid and dashed lines. (After Ref. 10.)

order) differ from calculation to calculation, there is general agreement that the highest occupied orbital in TTF is $4b_{1u}$, and that the lowest unoccupied (affinity) level in TCNQ is $3b_{2g}$, in the symmetry notation of Cotton.[18] The molecular orbitals for these two levels are shown in Figs. 4 and 5. Here constant wave-function contours are plotted in planes lying $\frac{1}{4}$ of the way between adjacent molecules in the TTF and TCNQ stacks in TTF-TCNQ, respectively. The contour serial numbers increase with increasing contour amplitude. These orbital pictures will prove useful in subsequent discussions. For further information about these contour plots, as well as additional plots depicting the orbital charge-density distributions in TTF and TCNQ, see Ref. 10.

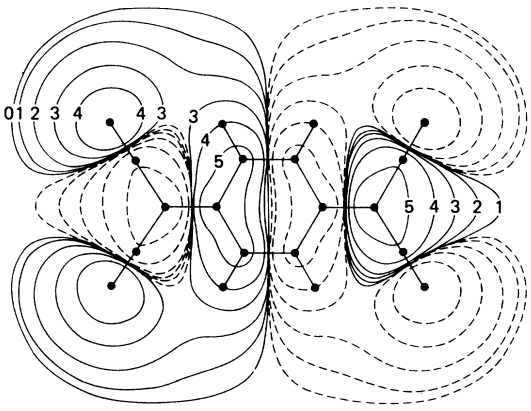

FIG. 5. $3b_{2g}$ molecular orbital for TCNQ, drawn in a plane $\frac{1}{4}$ of the way between successive molecules in a TCNQ chain in TTF-TCNQ. Positive and negative values are distinguished by solid and dashed lines. (After Ref. 10.)

B. Preliminary remarks concerning the band structure of TTF-TCNQ

As already noted, there is an average charge transfer of about 0.59 electron[17] from a TTF to a TCNQ molecule when these molecules come together to form crystalline TTF-TCNQ. This charge transfer is readily accounted for by an overlapping band model[26-29]: the TTF $4b_{1u}$ level gives rise to a valence band which overlaps the conduction band arising from the TCNQ $3b_{2g}$ level. Our calculations for the monomers and dimers of TTF and TCNQ clearly indicate that there are no other nearby TTF or TCNQ levels that give rise to energy bands which overlap the two energy bands just mentioned. It is sufficient, therefore, to discuss electronic-transport properties of TTF-TCNQ in terms of a two-band model.[26-29] We will not consider polaron effects[30] because these lie outside the scope of the present paper. However, it is instructive to point out that the electronic structure of TTF-TCNQ can also be described by localized molecular models[23,31] which stand in sharp contrast to the delocalized-band picture that is our primary concern here. According to these localized molecular models, the TTF and TCNQ chains are composed of TTF and TTF^+ molecules, and TCNQ and $TCNQ^-$ molecules, respectively. The proportions of neutral and charged species are determined by the average charge transfer. In both the localized and delocalized pictures, the intrachain transfer integrals, which we shall determine here, are of primary importance.

In the molecular models, it is necessary, in principle, to consider interactions between neutral neighbors, charged neighbors, and mixed neighbors, while in the band models it is sufficient to treat interactions between identically charged neighbors. Having established by previous calculations that the transfer integrals change only slightly with the state of charge of the molecules, we will restrict our attention here to the interactions between neutral neighbors.

Let us now consider the problem of estimating transfer integrals t and infinite-stack bandwidths W from dimer and trimer splittings (cf. Fig. 2). It is convenient to discuss this problem within the framework of the tight-binding approximation, which is appropriate to the narrow bands with which we are concerned. In the simplest tight-binding model characterized by the transfer or hopping integral t and the overlap integral S,[32] the eigenvalues for a polymer of length N units can be written in closed form[33] and are given by

$$E_l = \frac{2t\cos[l\pi/(N+1)]}{1+2S\cos[l\pi/(N+1)]}\ , \quad l=1,\ldots,N. \qquad (1)$$

The energy levels (with $S=0$) for a dimer and for a trimer are shown in Fig. 2, and the corresponding eigenvectors are indicated schematically in Fig. 3. For the infinite stack, the bandwidth W can be obtained from Eq. (1) by allowing $N\to\infty$ and taking the difference between the largest and smallest eigenvalues (i.e., E_1 and E_N, respectively). The result is

$$W=4t/(1-4S^2)\ . \qquad (2)$$

If one begins by calculating the dimer and trimer levels, it is possible to deduce the values of t and S separately and then to evaluate W. Of course, if one starts out with the monomer molecular orbitals, t and S can be computed directly so that the above discussion may seem somewhat academic. However, in scattered-wave calculations, it is not possible to determine t and S directly, so we are obliged to take the more circuitous route just described.

C. Previous work on TTF and TCNQ interchain interactions

There already exist many estimates of the TTF and TCNQ intrachain transfer integrals and bandwidths in TTF-TCNQ, as summarized in Table I. There are two disturbing aspects concerning these earlier estimates, most of which are based on semiempirical molecular-orbital calculations of various types.[19-23,28] In the first place, different methods or different parameterizations of the same method lead to strikingly different results. Secondly, changes in the basis set can also have profound effects on the calculated bandwidths. For example, in Ref. 20, the TTF bandwidth is found to be 0.72 or 0.20 eV, depending on whether d orbitals are included on the sulfur atoms. On the basis of the published material, it is difficult to assess the relative reliability of these several estimates. Before turning to our own work, we will briefly review some of these earlier estimates.

Ratner, Sabin, and Ball[34] were the first to perform detailed calculations on the interactions between TCNQ molecules. They used the semiempirical intermediate neglect of differential overlap (INDO) method to carry out calculations on TCNQ and its dimer in the geometry appropriate to NMP-TCNQ (*N*-methylphenazinium-TCNQ). This geometry is similar to that found in TTF-TCNQ. In NMP-TCNQ, one has the slipped, face-to-face stacking with an intermolecular distance of 3.22 Å, compared with 3.17 Å in TTF-TCNQ. The calculated transfer integral is 1.5 eV, which corresponds to a bandwidth of 6 eV if S is assumed to be negligible. This bandwidth is undoubtedly too large by an order of magnitude. (The similarity between

TABLE I. Previous theoretical estimates of intrachain transfer integrals t, dimer splittings Δ_2, and infinite-stack bandwidths W for TTF and TCNQ based on semiempirical calculations. The quantities actually calculated are shown without parentheses. Except as otherwise noted, parentheses encircle entries obtained by assuming $W=2\Delta_2=4t$. All entries are in eV.

Method	TTF t	TTF Δ_2	TTF W	TCNQ t	TCNQ Δ_2	TCNQ W	Ref.
INDO (Ratner *et al.*)				1.5		(6.0)	34
EH	0.05[a]		(0.20)	0.11		(0.44)	20
(Berlinsky *et al.*)		0.17[a]	(0.34)		0.35	(0.70)	
	0.18[b]		(0.72)				
EH (Tanaka *et al.*)				0.1377		(0.55)	23
CNDO-2			1.0			1.3–1.4	21
MINDO-2 (Ladik *et al.*)			(0.5)[c]			0.6	21

[a] No d orbitals used for sulfur atoms.
[b] d orbitals used for sulfur atoms.
[c] Scaled-down version of CNDO-2 result; not actually calculated.

TCNQ in NMP-TCNQ and TTF-TCNQ is underscored by the fact that in Ref. 23 Tanaka *et al.* find values of t of 0.1089 and 0.1377 for TCNQ in NMP-TCNQ and TTF-TCNQ, respectively.)

Berlinsky, Carolan, and Weiler[20] calculated the band-structure parameters for TTF-TCNQ, assuming tight-binding bands. They used the extended Huckel (EH) method to calculate the requisite matrix elements. For the TCNQ stack they found a transfer integral of 0.11 eV which corresponds to a bandwidth of 0.44 eV, assuming zero overlap integral. These same authors, using a different parameterization scheme, also calculated a dimer splitting for TCNQ of 0.35 eV (see discussion at the close of the second paper cited in Ref. 20). Since they found the overlap integrals to be quite small (0.02 and 0.03 between adjacent molecules on the TTF and TCNQ stacks, respectively), we can convert their dimer splitting of 0.35 eV into an infinite-stack bandwidth of 0.70 eV for TCNQ. Both of these estimates for the TCNQ bandwidth, 0.44 and 0.70 eV, are roughly consistent with experimental estimates of the total TTF-TCNQ bandwidth, which range from about 0.4 to 0.6 eV.[35,36]

Ladik *et al.*[21] have performed both CNDO-2 (complete neglect of differential overlap, version 2) and MINDO-2 (modified intermediate neglect of differential overlap, version 2) calculations for the TCNQ dimer and the band structure of an infinite TCNQ chain. The results are quite sensitive to the method used. With CNDO-2, the calculated bandwidth is 1.3–1.4 eV, depending on the charge state of the TCNQ molecule (or on the band filling), and 0.6 eV with the MINDO-2 method.

Let us now turn to the various estimates made for the bandwidth in TTF. Berlinsky, Carolan, and Weiler[20] obtained two different estimates of the TTF bandwidth, 0.72 and 0.20 eV, depending on whether d orbitals are included on the sulfur atoms. Using a different parameterization, they obtained a dimer splitting of 0.17 eV (no d orbitals on sulfur). Assuming $S=0$, this last value corresponds to a TTF bandwidth of 0.34 eV.

Ladik *et al.*[21] obtained a bandwidth of 1.0 eV for an infinite TTF chain using the CNDO-2 method. They were not able to obtain results for TTF by the MINDO-2 approach, but in the light of their TCNQ results, they scaled the CNDO-2 TTF result down by a factor of 2 to get an alternate estimate of 0.5 eV. As already noted, experimental estimates of the total TTF-TCNQ bandwidth range from about 0.4 to 0.6 eV.[35,36]

D. Present work on TCNQ and TTF dimers and trimers

Using various basis sets and atomic-sphere radii sets, we have carried out self-consistent and model scattered-wave calculations for TTF and TCNQ monomers, dimers, and trimers, as outlined above. Calculated dimer and trimer splittings (the latter divided by $\sqrt{2}$ in order to emphasize the smallness of the overlap integral) are listed in Table II for the TTF $4b_{1u}$ and TCNQ $3b_{2g}$ levels.

Our principal conclusions based on Table II are the following:

(a) For a given basis set, the model dimer splittings are slightly larger than the corresponding self-consistent dimer splittings for TTF. In the case of TCNQ, the model dimer splitting is about twice as large as the self-consistent dimer split-

TABLE II. Calculated values of dimer and trimer splittings for TTF ($4b_{1u}$ monomer) and TCNQ ($3b_{2g}$ monomer), according to the present work and Ref. 12. The trimer splittings Δ_3 are shown divided by $\sqrt{2}$ to emphasize their consistency with the dimer splittings on the assumption that the overlap integrals S are negligibly small. The bandwidths were determined by multiplying the dimer splittings by 2. Our best estimates are denoted by an asterisk. All entries are in eV.

		TTF			TCNQ		
Solution	Basis set	Δ_2	$\Delta_3/\sqrt{2}$	W	Δ_2	$\Delta_3/\sqrt{2}$	W
SCF[a]	Minimum	0.12		0.24	0.09		0.18
Model	Minimum	0.14	0.14	0.28	0.17	0.17	0.34
SCF	Intermediate	0.22		0.44			
Model	Intermediate	0.24		0.48			
Model	Extended	0.24	0.24	0.48*	0.29		0.58*

[a]SCF: Self-consistent field.

TABLE III. Orbital charge distributions for the $4b_{1u}$ TTF monomer level and related dimer and trimer levels. The energy eigenvalues, multiplied by -1, are also shown (in eV). In the dimers, the entries marked "average" are obtained by taking half the sum of the unprimed and primed atom values for b_u+a_g or half the corresponding int entry. Q(int) is denoted by int, and Q(atom) by atom, where atom is C 2, etc. Apparent discrepancies among corresponding entries of order 0.001 are usually due to roundoff.

	Orbital	int	C 2	C 2′	C 2″	S 3	S 3′	S 3″	C 4	C 4′	C 4″	$-\epsilon$ (eV)
Monomer, SCF, Minimum basis set	$4b_{1u}$	0.256	0.119			0.094			0.032			6.362
Dimer, SCF, Minimum basis set	b_u	0.233	0.062	0.042		0.042	0.056		0.017	0.025		9.090
	a_g	0.251	0.059	0.046		0.041	0.051		0.014	0.029		9.208
	b_u+a_g	0.484	0.121	0.088		0.083	0.107		0.031	0.054		
	Average	0.242	0.105			0.095			0.042			
Dimer, model Minimum basis set	b_u	0.243	0.061	0.057		0.049	0.049		0.018	0.014		6.293
	a_g	0.263	0.058	0.061		0.046	0.046		0.015	0.018		6.436
	b_u+a_g	0.506	0.119	0.118		0.095	0.095		0.032	0.032		
	Average	0.253	0.119			0.095			0.032			
Monomer, SCF, Intermediate basis set	$4b_{1u}$	0.261	0.106			0.106			0.025			5.457
Dimer, model, Intermediate basis set	b_u	0.242	0.056	0.051		0.057	0.054		0.014	0.012		5.326
	a_g	0.271	0.050	0.055		0.051	0.053		0.011	0.014		5.569
	b_u+a_g	0.513	0.106	0.106		0.108	0.107		0.025	0.026		
	Average	0.257	0.106			0.107			0.025			
Dimer, SCF, Intermediate basis set	b_u	0.234	0.058	0.041		0.053	0.059		0.014	0.016		7.110
	a_g	0.260	0.053	0.046		0.049	0.057		0.011	0.019		7.328
	b_u+a_g	0.494	0.111	0.087		0.102	0.116		0.025	0.035		
	Average	0.247	0.099			0.109			0.030			
Monomer, SCF, Extended basis set	$4b_{1u}$	0.270	0.101			0.100			0.032			5.00
Dimer, model Extended basis set	b_u	0.251	0.053	0.043		0.053	0.051		0.018	0.015		4.867
	a_g	0.279	0.048	0.052		0.049	0.052		0.014	0.018		5.103
	b_u+a_g	0.530	0.101	0.100		0.102	0.103		0.032	0.033		
Trimer, model, Extended basis set	b_u	0.243	0.027	0.052	0.023	0.026	0.055	0.025	0.009	0.017	0.007	4.812
	a_g	0.265	0.050	0.0	0.050	0.051	0.0	0.050	0.016	0.0	0.016	4.983
	b_u	0.284	0.024	0.047	0.027	0.025	0.048	0.026	0.007	0.015	0.009	5.147
	$b_u+a_g+b_u$	0.792	0.101	0.099	0.100	0.102	0.103	0.101	0.032	0.032	0.032	

TABLE IV. Orbital charge distributions for $3b_{2g}$ TCNQ monomer level and related dimer and trimer levels.

Case	Orbital	int	C 2	C 2′	C 2″	C 3	C 3′	C 3″	C 4	C 4′	C 4″	C 5	C 5′	C 5″	N 6	N 6′	N 6″	$-\epsilon$ (eV)
Monomer, SCF, minimum basis set	$3b_{2g}$	0.264	0.029			0.072			0.165			0.0			0.036			9.33
Dimer, SCF, minimum basis set	b_u	0.234	0.015	0.014		0.026	0.030		0.092	0.097					0.019	0.020		15.242
	a_g	0.238	0.015	0.012		0.021	0.026		0.100	0.089					0.023	0.022		15.331
	b_u+a_g	0.472	0.030	0.026		0.047	0.056		0.192	0.186					0.042	0.042		
	Average	0.236	0.028			0.051			0.189			0.0	0.0		0.042			
Dimer, model, minimum basis set	b_u	0.271	0.014	0.016		0.040	0.039		0.074	0.086					0.016	0.017		9.241
	a_g	0.280	0.015	0.012		0.032	0.033		0.089	0.077					0.020	0.018		9.413
	b_u+a_g	0.551	0.029	0.028		0.072	0.072		0.163	0.163		0.0	0.0		0.036	0.035		
Trimer, model, minimum basis set	a_g	0.268	0.007	0.016	0.008	0.020	0.042	0.020	0.035	0.081	0.043				0.007	0.016	0.008	9.200
	b_u	0.276	0.014	0.0	0.014	0.086	0.0	0.036	0.081	0.0	0.081				0.018	0.0	0.018	9.329
	a_g	0.281	0.008	0.013	0.006	0.016	0.030	0.016	0.047	0.081	0.039				0.011	0.019	0.009	9.443
	$a_g+b_u+a_g$	0.825	0.029	0.029	0.028	0.072	0.072	0.072	0.163	0.162	0.163	0.0	0.0	0.0	0.036	0.035	0.035	
Monomer, SCF, extended basis set	$3b_{2g}$	0.285	0.032			0.094			0.110			0.013			0.031			7.434
Dimer, model, extended basis set	b_u	0.275	0.015	0.019		0.053	0.052		0.046	0.060		0.006	0.008		0.013	0.015		7.302
	a_g	0.291	0.017	0.014		0.043	0.044		0.065	0.050		0.007	0.006		0.018	0.015		7.590
	b_u+a_g	0.566	0.032	0.033		0.096	0.096		0.111	0.110		0.013	0.014		0.031	0.030		

ting when minimum basis sets are used. The difference in behavior is also reflected in the larger charge redistribution produced by dimer formation in TCNQ than in TTF (cf. Tables III and IV).

(b) The dimer splittings are consistently larger for extended basis sets than for minimum basis sets. In the case of TTF, the inclusion of d partial waves on the sulfur atoms leads to nearly the same splitting as inclusion of such waves on all the sulfur and carbon atoms. Since the extended basis-set solutions are more accurate than the minimum basis-set solutions, we will favor the former over the latter. The present results suggest that extended basis sets should be used in similar calculations on other dimer systems.

(c) By comparing the dimer and trimer splittings, we find that the intrachain overlap integrals S are negligible for the levels of interest. Accordingly, we can obtain t by dividing the dimer splitting by 2 and W by multiplying the dimer splitting by 2.

Let us now turn to the distribution of electronic charge in the bonding and antibonding dimer orbitals arising from TTF $4b_{1u}$ and TCNQ $3b_{2g}$, and to the corresponding trimer orbitals. The clearest way to see the charge distribution is to examine molecular-orbital contour maps, which are given for the dimer orbitals of TTF in Fig. 6. These maps are based on the intermediate basis-set self-consistent calculation for the TTF dimer. The bonding a_g orbitals are shown at the left, the antibonding b_u orbitals at the right. The upper panels show the molecular orbitals in the equatorial plane, and the lower panels show the contours in a plane lying perpendicular to the monomer planes and passing through the C 2 and C 2′ atoms.

A careful study of these dimer orbital plots provides some insight into why extended basis sets lead to larger dimer splittings than minimum basis sets. It is clear from Fig. 6 that the bonding and antibonding orbitals are quite intricate because of the fact that the underlying TTF $4b_{1u}$ orbital already has considerable nodal structure of its own. By using d partial waves in addition to s and p partial waves, it is possible to obtain more faithful solutions for the bonding and antibonding orbitals, including the distinctions between them. With the d orbitals included, the "parent" monomer charge distributions can become more asymmetrical in the dimer with respect to their respective monomer planes than would be possi-

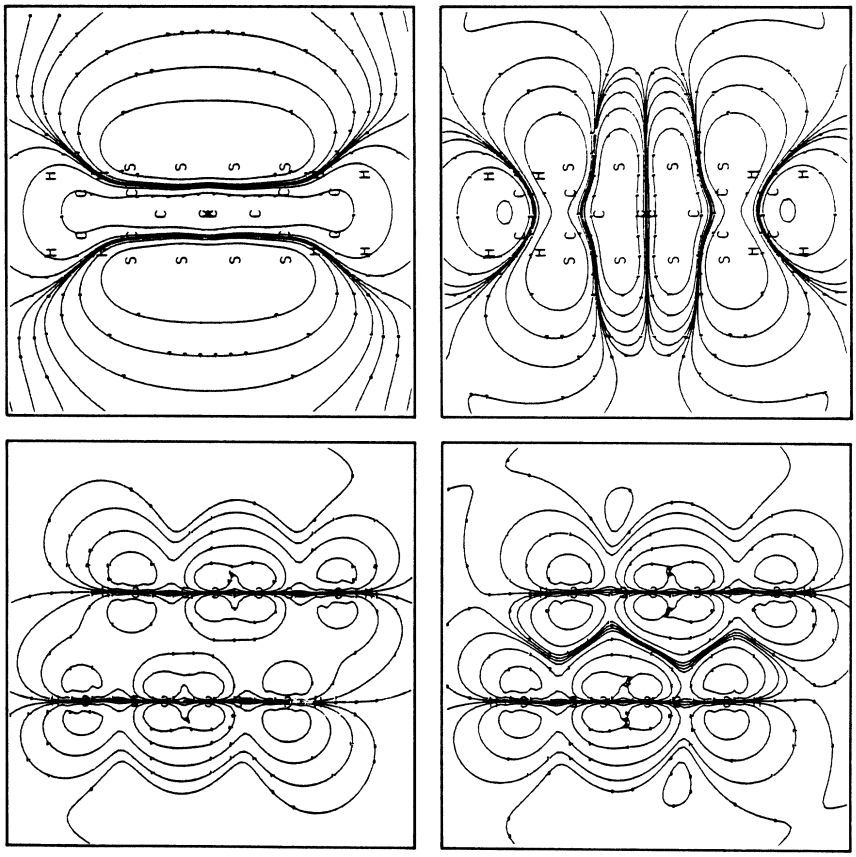

FIG. 6. Molecular-orbital contours for the a_g and b_u levels in the TTF dimer. Positive and negative contours are not distinguished explicitly, but can be inferred from the nodal structure. The bonding a_g level arising from TTF b_{1u} is shown at the left, and the antibonding b_u level at the right. The upper panels show the contours in the equatorial plane, and the lower panels the contours in a plane lying perpendicular to the monomers and passing through the C2 and C2′ atoms. The ratio of successive contour magnitudes is 3.16 [$=(10)^{1/2}$].

ble otherwise.

Within the context of scattered-wave calculations, we may define a "balanced" basis set as one composed of all the partial waves analogous to the occupied valence orbitals, such as s and p on carbon and sulfur and only s on hydrogen, or of all these plus one additional partial wave (polarization term) on each atom. The former corresponds to our minimum basis set, and the latter to our extended basis set. We do not regard our intermediate basis set (with d partial waves on sulfur but not on carbon) as a balanced basis set because it provides a more detailed description of the sulfur than the carbon environments. In our work the intermediate basis leads to a solution for the TTF dimer considerably closer to the extended than the minimum basis solution, indicating the greater importance of the sulfur atoms in the dimer formation. It is possible that the large difference between the calculated dimer splittings obtained in Ref. 20 with and without d orbitals on the sulfur atoms, is a manifestation of an "unbalanced" basis-set effect, that is to say, the sulfur atoms are given undue influence.

Let us now look into the charge distributions on TTF and TCNQ monomers, dimers, and trimers in somewhat greater detail. For this purpose it is convenient to list for each molecular orbital the charges contained inside each inequivalent atomic sphere, Q(atom), where atom is C 2, C 3, etc., as well as inside the intersphere region, Q(int). This information, which is provided directly by scattered-wave calculations,[8-12] is listed for key TTF and TCNQ solutions in Tables III and IV. In order to conserve space we have not listed the hydrogen spheres or the outer sphere regions, which contain negligible charge for the cases of interest. For monomers and dimers, the atomic labeling follows Fig. 1. For trimers, the unprimed and doubly primed atoms refer to the top or bottom monomer, while the singly primed atoms refer to the central monomer, for which corresponding right and left atoms (in Fig. 1) have the same charge contents.

In examining Tables III and IV, it should be borne in mind that the various Q(atom) are merely indicative of the orbital charge distribution, since these quantities represent only about $\frac{3}{4}$ of the total orbital charge when they are weighted according to the number of atoms of each type and summed over all types. The remaining $\frac{1}{4}$ or so of an electron charge (per orbital) is represented by Q(int), the intersphere charge content. Even though the charge in the intersphere region cannot be assigned to individual atoms—Q(int) describes a common pool—it is still possible to gain considerable insight into the nature of the charge distributions from a careful study of the Q(atoms)'s.

Let us now consider Table III, beginning at the top, where we show the minimum basis set TTF monomer and dimer self-consistent solutions. In going from a self-consistent monomer to the self-consistent dimer, the principle charge redistribution arises from the inequivalence of conjugate (unprimed and primed) atoms inherent in the C_{2h} symmetry of the dimer. This dimer-induced asymmetry is considerably larger than the average charge transfer from one pair of conjugate atoms, say, C 2 and C 2′, to another pair, say S 3 and S 3′. This can be seen by comparing the average Q(atom) for such a pair with the Q(atom) of the parent monomer atom: the former is nearly equal to the latter.

The principal effect of going to the intermediate basis set (adding d partial waves to the sulfur atoms only) is to place more charge on the sulfur atoms at the expense of the carbon atoms. When d partial waves are added to the carbon atoms as well (extended basis set), the C 2 and S 3 atoms and their conjugates lose charge, while the C 4 atom and its conjugate gain charge. The net effect is only a slight increase in the dimer splitting.

There is considerably more charge redistribution produced by dimer formation in TCNQ than in TTF, judging by the self-consistent monomer and dimer entries. This must mean that the TCNQ dimer orbitals are concentrated in a region which has a greater asymmetry than the corresponding regions for the TTF dimer orbitals. In the case of the model dimer and trimer solutions, we see that there is a slight charge transfer between conjugate atoms for a given orbital, but the sum of the charges for the two levels in the dimer (or the three levels in the trimer) is the same as the parent monomer atomic charge. In other words, there is no net charge transfer between conjugate atoms in the model dimers and trimers, as is to be expected from their construction.

It is clear that self-consistent dimer solutions are more appropriate to isolated dimers in solution or in special crystal structures than for adjacent molecules in uniformly spaced infinite stacks. When such stacks are formed from free monomers, we can expect some charge redistribution to take place, but this charge redistribution should be considerably smaller than that taking place when isolated dimers are formed from free monomers. For an isolated dimer, the region between the monomers is markedly different from the regions above and below, as is evident from Fig. 6. The inequivalence of the central and outer regions is responsible for much of the charge transfer between conjugate atoms, which in an isolated dimer have quite different environ-

ments.

On the other hand, in an infinite stack any given monomer will have environments above and below that are more similar to one another than they would be if the monomer belonged to an isolated dimer. These two environments are identical when the stacking is fully eclipsed (D_{2h}). For TTF-TCNQ, where the stacking is staggered (C_{2h}), the charge distributions associated with conjugate atoms are identical in content but different in orientation. This difference in orientation leads to a stack-induced asymmetry for each monomer in the stack.

If we take the view that stack formation leads to considerably less charge redistribution than isolated dimer formation, then adjacent molecules in infinite uniformly spaced stacks should be more nearly represented by our model than by our self-consistent dimer solutions. This is the view that we will adopt. Accordingly, we consider our model extended-basis-set solutions as our best solutions for TTF-TCNQ.

It is gratifying that this turns out to be the case because it is considerably easier to carry out model calculations than self-consistent ones. It is also noteworthy that in the present context, a suitably chosen model (frozen monomers) is more realistic than the corresponding self-consistent solution. It is additonally gratifying that our best dimer and trimer solutions (model, extended basis set) lead to bandwidths for TTF and TCNQ chains of 0.5 and 0.6 eV, respectively. These values are consistent with current experimental estimates of 0.4–0.6 eV for the total TTF-TCNQ bandwidth.[35,36] The corresponding transfer integrals are applicable to localized molecular models for TTF-TCNQ[23,31] as well as to delocalized band-structure models.

E. Band structure of TTF-TCNQ: additional remarks

We showed earlier, in Fig. 2, the relationship between the energy-level structures of monomers, dimers..., and infinite stacks. At the bottom of this figure we show the valence and conduction bands for the TTF and TCNQ chains in TTF-TCNQ. Since there appears to be some confusion (as noted at recent conferences) about the reason why the TTF and TCNQ bands have opposite shapes, we will discuss this point briefly.

In order to determine whether the band maximum lies at the zone center or at the zone edge, it is necessary to look at the dimer orbitals (or at a linear combination of suitably arranged monomer orbitals). This is done for the two bands of principal interest in Fig. 7.

Here we show, schematically, the phases of the

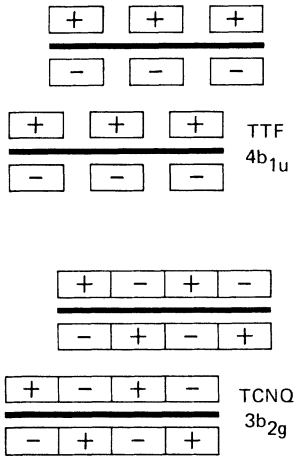

FIG. 7. Schematic diagram of successive monomer orbitals on infinite TTF and TCNQ stacks. Both pictures represent Bloch functions with $k=0$ (Fig. 2). The upper diagram corresponds to the TTF dimer b_u antibonding orbital, which is shown more realistically in the lower right-hand panel of Fig. 6. The lower diagram corresponds to the TCNQ dimer a_g bonding oribtal.

monomer orbitals in the plane perpendicular to the monomers and passing through the C 2 and C 2′ atoms in TTF and the C 3, C 4, and C 3′, and C 4′ atoms in TCNQ (cf. Fig. 1). We have placed the same monomer orbital on each member of an infinite stack to represent the $k=0$ Bloch function. In the case of TTF, the phases are such that our $k=0$ Bloch function corresponds to an antibonding or b_u dimer orbital, so this must lie higher in energy than the corresponding bonding or a_g dimer orbital, which can be obtained by reversing all the signs in the lower TTF monomer, but, of course, this change of sign corresponds to reversing the sign of every other monomer in an infinite stack, i.e., to a zone-edge Bloch function. The same conclusion is reached if one samples the monomer orbitals in other planes lying parallel to the one already treated. For this purpose TTF monomer orbital shown in Fig. 4 comes in handy. Repeating the same argument for TCNQ (and using the TCNQ monomer orbital shown in Fig. 5), one reaches the opposite conclusion for the TCNQ chain, i.e., the band maximum lies at the zone edge rather than at the zone center.

In short, the different shapes of the TTF and TCNQ energy bands are a direct consequence of the different symmetries of the monomer orbitals and the different phase relationships exhibited by successive monomer orbitals in a stack. It is clear from Fig. 7, for example, that if we used the same orbitals and went from staggered stacking to eclipsed stacking, the band shape would re-

main the same for TTF but would reverse for TCNQ.

IV. CONCLUSION

In this paper we have shown how intrachain transfer integrals and infinite-stack bandwidths for the TTF and TCNQ stacks in TTF-TCNQ can be determined by carrying out model (non-self-consistent) $X\alpha$ scattered-wave calculations. Self-consistent dimer calculations, which describe isolated dimers more closely than adjacent molecules in an infinite stack, lead to dimer splittings that are smaller than those given by model (non-self-consistent) calculations. The individual-stack bandwidths calculated with extended basis sets are consistent with experimental estimates of the total TTF-TCNQ bandwidth. If minimum basis sets are used, the calculated bandwidths are found to be considerably smaller. In view of the quantitative success of these calculations for TTF and TCNQ, we are encouraged to attempt similar studies of other charge-transfer complexes. Results of calculations for tetraselenafulvalene (TSeF) dimers (in pure TSeF and in TSeF-TCNQ) will be reported elsewhere.[37]

ACKNOWLEDGMENTS

The authors are grateful to Dr. P. M. Grant, Dr. J. J. Ritsko, Dr. W. E. Rudge, and Dr. J. B. Torrance for stimulating discussions.

APPENDIX: CHOICE OF ATOMIC RADII FOR TCNQ

Some of the TCNQ calculations were carried out using atomic-sphere radii determined by the Norman criterion.[38] As a first step in determining the molecular charge distribution, free-atom charge distributions are placed at the various atomic positions in the molecule, and the spherically averaged charge distribution, with respect to each atomic position, is calculated. With this information in hand, it is possible to calculate the total charge enclosed by a sphere of arbitrary radius centered at each atomic position. According to Norman, the atomic-sphere radii to be used in scattered-wave calculations should be proportional to the radii of the atomic spheres which contain the atomic number of electrons for each atom, e.g., six for carbon, seven for nitrogen, etc. In order to establish the proportionality factor, the radii are first chosen so that they describe the largest possible set of nonoverlapping atomic spheres. Then, all of these radii are increased by a constant factor of about 1.3 to establish a reasonable degree of overlap. This approach has been used successfully in a variety of applications.[39]

If this simple scheme is applied to the TCNQ molecule, it leads to a reasonable overlap between the C and N spheres on the cyano groups, but to unacceptably small overlaps elsewhere. This is a consequence of the fact that the CN triple-bond length is considerably smaller than CC double- and CC single-bond lengths elsewhere on the molecule. In order to obtain reasonable overlaps over most of the molecule, we used a scaling factor of 1.4 rather than 1.3. The radii calculated in this manner are 1.56, 1.54, 1.54, 1.49, 1.56, and 1.15 bohr for C 2, C 3, C 4, C 5, N 6, and H 7, respectively. This leads to excessive overlap between the C and N spheres on the cyano groups, a situation whose consequences have been discussed at length in Ref. 9. In the present application, this excessive overlap is of minor importance because it has negligible effect on the $TCNQ^0$ affinity level (the level of principal interest here) and neighboring levels. In contrast to our earliest work on TTF and TCNQ monomers based on overlapping spheres,[8-10] our more recent work[11,12] includes overlap corrections which prevent double counting of charge in the overlap regions, and thereby offset the effects of excessive overlap.

The second set of atomic radii used for TCNQ are the same as those used in the second paper listed under Ref. 8. The radii for C 2, C 3, C 4, and H 7 are so chosen that the volumes of the atomic spheres are 2.1 times as large as the corresponding nonoverlapping atomic spheres for the neutral TCNQ monomer. For C 5 and N 6 (the cyano group), the volume ratio is 3.0 rather than 2.1.

---

*Present address: Département de Chimie, Université de Montréal, Montréal, Canada H3C 3V1.

[1] *Chemistry and Physics of One-Dimensional Metals*, edited by H. J. Keller (Plenum, New York, 1977); Proceedings of the NATO Advanced Study Institute, Bolzano, Italy, 1976 (unpublished).

[2] K. Krogmann, in Ref. 1, and references cited therein.

[3] Cf. Ref. 1, particularly the review articles by A. N. Bloch; R. Comès; A. J. Heeger, D. Jerome and M. Weger, and J. Torrance.

[4] R. L. Greene and G. B. Street, in Ref. 1, and references cited therein.

[5] For additional references, see *Low Dimensional Cooperative Phenomena*, edited by H. J. Keller (Plenum, New York, 1975); Proceedings of the Conference on Organic Conductors and Semiconductors, Siófok, Hungary, 1976 (unpublished).

[6] L. V. Interrante and R. P. Messmer, Inorg. Chem.

1174 (1971).
[7]R. P. Messmer and D. R. Salahub, Phys. Rev. Lett. 35, 533 (1975).
[8]F. Herman, Nuovo Cimento B 23, 282 (1974); Phys. Rev. Lett. 33, 94 (1974); B. I. Bennett and F. Herman, Chem. Phys. Lett. 32, 334 (1975); I. P. Batra, B. I. Bennett, and F. Herman, Phys. Rev. B 11, 4927 (1975).
[9]F. Herman, A. R. Williams, and K. H. Johnson, J. Chem. Phys. 61, 3508 (1974); K. H. Johnson, F. Herman, and R. Kjellander, in *Electronic Structure of Polymers and Molecular Crystals*, edited by J. Andrê, J. Ladik, and J. Delhalle (Plenum, New York, 1975), p. 601.
[10]F. Herman, W. E. Rudge, I. P. Batra, and B. I. Bennett, Intern. J. Quantum Chem. 10S, 167 (1976).
[11]F. Herman, in *Electrons in Finite and Infinite Structures*, edited by P. Phariseau (Plenum, New York, 1977).
[12]D. R. Salahub, R. P. Messmer, and F. Herman, Phys. Rev. B 13, 4252 (1976).
[13]D. R. Salahub and R. P. Messmer, J. Chem. Phys. 64, 2039 (1976).
[14]R. P. Messmer and D. R. Salahub, Chem. Phys. Lett. 41, 73 (1976); D. R. Salahub and R. P. Messmer, Phys. Rev. B 14, 2592 (1976).
[15]R. Foster, *Organic Charge-Transfer Complexes*, (Academic, London, 1969); F. H. Herbstein, in *Perspectives in Structural Chemistry*, edited by J. D. Duntz and J. A. Ibers (Wiley, New York, 1971), Vol. 4, p. 166; R. P. Shibaeva and L. O. Atovmyan, Zh. Strukt. Khim. 13, 546 (1972). English translation available from Consultants Bureau, Plenum, New York.
[16]T. J. Kistenmacher, T. E. Phillips, and D. O. Cowan, Acta Crystallogr. B 30, 763 (1974).
[17]P. Coppens, Phys. Rev. Lett. 35, 98 (1975); F. Denoyer, F. Comès, A. F. Garito, and A. J. Heeger, *ibid.* 35, 445 (1975); R. Comès, S. M. Shapiro, G. Shirane, A. F. Garito, and A. J. Heeger, *ibid.* 35, 1518 (1975); Phys. Rev. B 14, 2376 (1976).
[18]F. A. Cotton, *Group Theory with Chemical Applications*, 2nd ed. (Wiley-Interscience, New York, 1971).
[19]D. A. Lowitz, J. Chem. Phys. 46, 4698 (1967); S. Hiroma, H. Kuroda, and H. Akamatu, Bull. Chem. Soc. Jpn. 44, 9 (1971); H. T. Jonkman and J. Kommandeur, Chem. Phys. Lett. 15, 496 (1972); A. Bieber and J. J. Andre, Chem. Phys. 5, 166 (1974).
[20]A. J. Berlinsky, J. F. Carolan, and L. Weiler, Solid State Commun. 15, 795 (1974); 19, 1165 (1976).
[21]J. Ladik, A. Karpfen, G. Stollhoff, and P. Fulde, Chem. Phys. 7, 267 (1975); A. Karpfen, J. Ladik, G. Stollhoff, and P. Fulde, *ibid.* 8, 215 (1975); J. Ladik, Intern. J. Quantum Chem. 9, 563 (1975).
[22]N. O. Lipari, P. Nielsen, J. J. Ritsko, A. J. Epstein, and D. J. Sandman, Phys. Rev. B 14, 2229 (1976).
[23]J. Tanaka, M. Tanaka, T. Kawai, T. Takabe, and O. Maki, Bull. Chem. Soc. Jpn. 49, 2358 (1976).
[24]H. T. Jonkman, G. A. Van der Velde, and W. C. Nieuwpoort, Chem. Phys. Lett. 25, 62 (1974).
[25]H. Johansen, Intern. J. Quantum Chem. 9, 459 (1975).
[26]M. H. Cohen, J. A. Hertz, P. M. Horn, and V. K. S. Shante, Intern. J. Quantum Chem. 8S, 491 (1974).
[27]U. Bernstein, P. M. Chaikin, and P. Pincus, Phys. Rev. Lett. 34, 271 (1975).
[28]A. J. Berlinsky, Contemp. Phys. 17, 331 (1976).
[29]D. Jerome and M. Weger, in Ref. 1.
[30]K. Krogh-Jespersen and M. A. Ratner, Chem. Phys. Lett. 39, 123 (1976), and references cited therein.
[31]J. B. Torrance, in Ref. 1.
[32]See, for example, F. L. Piler, *Elementary Quantum Chemistry* (McGraw-Hill, New York, 1968).
[33]R. P. Messmer, Phys. Rev. B 15, 1811 (1977).
[34]M. A. Ratner, J. R. Sabin, and E. E. Ball, Mol. Phys. 26, 1177 (1974).
[35]J. B. Torrance (private communication); and B. Welber and P. M. Grant (unpublished). The latter authors have analyzed optical reflectivity spectra for TTF-TCNQ with a view to determining the TTF and TCNQ bandwidths. Using the experimental value of the plasma edge, 1.26 eV, and assuming a TCNQ bandwidth of 0.5 eV, they deduce a TTF bandwidth of approximately 0.5 eV.
[36]J. J. Ritsko, D. J. Sandman, A. J. Epstein, P. C. Gibbons, S. E. Schnatterly, and J. Fields, Phys. Rev. Lett. 34, 1330 (1975), and references cited therein; J. J. Ritsko, N. O. Lipari, P. C. Gibbons, and S. E. Schnatterly, *ibid.* 37, 1068 (1976).
[37]F. Herman (unpublished).
[38]J. G. Norman, Jr., J. Chem. Phys. 61, 4630 (1974).
[39]J. G. Norman, Jr., J. Am. Chem. Soc. 33, 97 (1975); 33, 3833 (1975); 33, 6596 (1975).

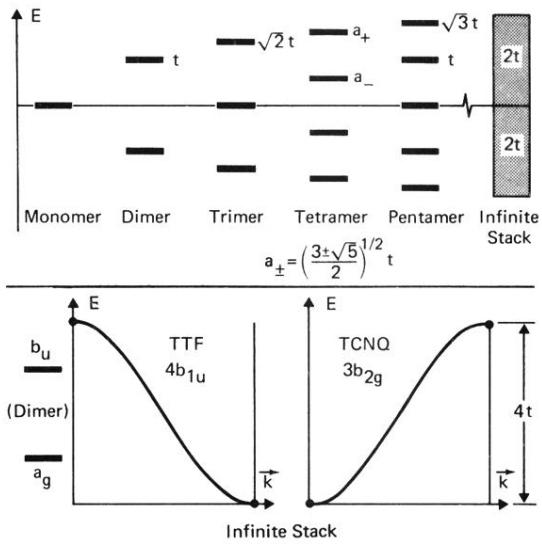

FIG. 2. Comparison of energy levels for monomers, dimers, trimers, etc., indicating their relationship to the energy-level spectrum of an infinite stack. In the upper panel, t denotes the transfer integral, and S, the overlap integral, has been set equal to zero. The band structures of infinite TTF and TCNQ stacks are shown in the lower panel.